J|A|C|S
ARTICLES
Published on Web 03/13/2004

Oxidation and Oxygenation of Iron Complexes of 2-Aza-21-carbaporphyrin

Krystyna Rachlewicz,[†] Sian-Ling Wang,[‡] Jia-Ling Ko,[‡] Chen-Hsiung Hung,[‡]* and Lechosław Latos-Grażyński[†]*

Contribution from the Department of Chemistry, University of Wrocław, 14 F. Joliot-Curie St., Wrocław 50 383, Poland, and Department of Chemistry, National Changhua University of Education, Changhua, 50058 Taiwan

Received November 25, 2003; E-mail: llg@wchuwr.chem.uni.wroc.pl; chhung@cc.ncue.edu.tw

Abstract: Oxidation and oxygenation of (*H*CTPP*H*)Fe^{II}Br an iron(II) complex of 2-aza-5,10,15,20-tetraphenyl-21-carbaporphyrin (CTPP*H*)H_2 have been followed by ^{1}H and ^{2}H NMR spectroscopy. Addition of I_2 or Br_2 to the solution of (*H*CTPP*H*)Fe^{II}Br in the absence of dioxygen results in one-electron oxidation yielding [(*H*CTPP*H*)Fe^{III}Br]$^+$. One electron oxidation with dioxygen, accompanied by deprotonation of a C(21)H fragment and formation of an Fe−C(21) bond, produces an intermediate-spin, five-coordinate iron(III) complex (*H*CTPP)Fe^{III}Br. In the subsequent step an insertion of the oxygen atom into the preformed Fe^{III}−C(21) bond has been detected to produce [(CTPP*O*)Fe^{III}Br]$^-$. Protonation at the N(2) atom affords (*H*CTPP*O*)Fe^{III}Br. The considered mechanism of (*H*CTPP*H*)Fe^{II}Br oxygenation involves the insertion of dioxygen into the Fe−C bond. The ^{1}H NMR and ^{2}H NMR spectra of paramagnetic iron(III) complexes were examined. Functional group assignments have been made with use of selective deuteration. The characteristic patterns of pyrrole and 2-NH resonances have been found diagnostic of the ground electronic state of iron and the donor nature localized at C(21) center as exemplified by the ^{1}H NMR spectrum of intermediate-spin (*H*CTPP)Fe^{III}Br: β-H 7.2, −10.6, −19.2, −20.6, −23.2, −24.9, −43.2; 2-NH −76.6 (ppm, 298 K). The structures of two compounds (*H*CTPP)Fe^{III}Br and (*H*CTPP*O*)Fe^{III}Br, were determined by X-ray diffraction studies. In the first case, the iron(III) is five-coordinate with bonds to three pyrrole nitrogen atoms (Fe−N distances: 1.985(8), 2.045(7), 2.023(8) Å), and the pyrrolic trigonal carbon (Fe−C: 1.981(8) Å). The iron(III) of (*H*CTPP*O*)Fe^{III}Br forms bonds to three pyrrole nitrogen atoms (Fe−N distances 2.104(5), 2.046(5), 2.102(5) Å). The Fe−O 2.041(5) Å and Fe−C(21) 2.192(5) Å distances suggests a direct interaction between the iron center and the π electron density on the carbonyl group in a η^2 fashion.

Introduction

Inverted (*N*-confused) porphyrin 5,10,15,20-tetraaryl-2-aza-21-carbaporphyrin (CTPP*H*)H_2 and its derivatives[1−3] revealed a remarkable tendency to stabilize peculiar organometallic compounds,[4−6] containing diamagnetic nickel(II),[1,7−11] paramagnetic nickel(II) with one or two Ni−C bonds,[12,13] nickel(III),[11,14,15] copper(II),[16,17] copper(III),[18] palladium(II),[19] antimony(V),[20] silver(III),[17,21] manganese(II) and manganese(III),[22,23] zinc(II),[16,24] iron,[25,26] rhodium(I),[27] and platinum.[28] An accompanying involvement of the perimeter nitrogen atom which results in the outer coordination has been detected for iron-

[†] University of Wrocław.
[‡] National Changhua University of Education.

(1) Chmielewski, P. J.; Latos-Grażyński, L.; Rachlewicz, K.; Głowiak, T. *Angew. Chem., Int. Ed. Engl.* **1994**, *33*, 779.
(2) Furuta, H.; Asano, T.; Ogawa, T. *J. Am. Chem. Soc.* **1994**, *116*, 767.
(3) We will use the symbol CTPP to denote the trianion obtained from the inverted porphyrin by abstraction of all pyrrolic NH proton and the C-bound H(21) hydrogen. The groups attached to the N(2) atom will be indicated by a prefix in italic and the group attached to C(21) will appear as a suffix in italic. A similar methods will be used to form acronyms for other carbaporphynoids.
(4) Latos-Grażyński, L. Core Modified Heteroanalogues of Porphyrins and Metalloporphyrins; In *The Porphyrin Handbook*; Kadish, K. M., Smith, K. M., Guilard, R., Eds.; Academic Press: New York, 2000; pp 361−416.
(5) Furuta, H.; Maeda, H.; Osuka, A. *Chem. Commun.* **2002**, 1795.
(6) Harvey, J. D.; Ziegler, C. J. *Coord. Chem. Rev.* **2003**, *247*, 1.
(7) Chmielewski, P. J.; Latos-Grażyński, L. *J. Chem. Soc., Perkin Trans.2* **1995**, 503.
(8) Lash, T. D.; Richter, D. T.; Shiner, C. M. *J. Org. Chem.* **1999**, *64*, 7973.
(9) Xiao, Z.; Patrick, B. O.; Dolphin, D. *Chem. Commun.* **2002**, 1816.
(10) Schmidt, I.; Chmielewski, P. J.; Ciunik, Z. *J. Org. Chem.* **2002**, *67*, 8917.
(11) Schmidt, I.; Chmielewski, P. J. *Inorg. Chem.* **2003**, *42*, 5579.
(12) Chmielewski, P. J.; Latos-Grażyński, L.; Głowiak, T. *J. Am. Chem. Soc.* **1996**, *118*, 5690.
(13) Chmielewski, P. J.; Latos-Grażyński, L. *Inorg. Chem.* **2000**, *39*, 5639.
(14) Chmielewski, P. J.; Latos-Grażyński, L. *Inorg. Chem.* **1997**, *36*, 840.
(15) Xiao, Z.; Patrick, B. O.; Dolphin, D. *Inorg. Chem.* **2003**, *42*, 8125.
(16) Chmielewski, P. J.; Latos-Grażyński, L.; Schmidt, I. *Inorg. Chem.* **2000**, *39*, 5475.
(17) Maeda, H.; Osuka, A.; Ishikawa, Y.; Aritome, I.; Hisaeda, Y.; Furuta, H. *Org. Lett.* **2003**, *5*, 1293.
(18) Maeda, H.; Ishikawa, Y.; Matsuda, T.; Osuka, A.; Furuta, H. *J. Am. Chem. Soc.* **2003**, *125*, 11822.
(19) Furuta, H.; Kubo, N.; Maeda, H.; Ishizuka, T.; Osuka, A.; Nanami, H.; Ogawa, T. *Inorg. Chem.* **2000**, *39*, 5424.
(20) Ogawa, T.; Furuta, H.; Takahashi, M.; Morino, A.; Uno, H. *J. Organometallic Chem.* **2000**, *611*, 551.
(21) Furuta, H.; Ogawa, T.; Uwatoko, Y.; Araki, K. *Inorg. Chem.* **1999**, *38*, 2676.
(22) Harvey, J. D.; Ziegler, C. J. *Chem. Commun.* **2002**, 1942.
(23) Bohle, D. S.; Chen, W.-C.; Hung, C.-H. *Inorg. Chem.* **2002**, *41*, 3334.
(24) Furuta, H.; Ishizuka, T.; Osuka, A. *J. Am. Chem. Soc.* **2002**, *124*, 5622.
(25) Chen, W.-C.; Hung, C.-H. *Inorg. Chem.* **2001**, *40*, 5070.
(26) Hung, C.-H.; Chen, W.-C.; Lee, G.-H.; Peng, S.-M. *Chem. Commun.* **2002**, 1516.
(27) Srinivasan, A.; Furuta, H.; Osuka, A. *Chem. Commun.* **2001**, 1666.
(28) Furuta, H.; Youfu, K.; Maeda, H.; Osuka, A. *Angew. Chem., Int. Ed. Engl.* **2003**, *42*, 2186.

 10.1021/ja039792y CCC: $27.50

(II),[26] palladium(II),[19] and platinum(II) complexes.[28] The related carbaporphyrinoid, i.e., the pyrrole append *O*-confused oxacarbaporphyrin gave three structurally related organometallic complexes with nickel(II), palladium(II) and silver(III) in which the metal ions are bound by three pyrrolic nitrogens and a trigonally hybridized C(21) atom of the *O*-confused furan.[29] A stable aromatic silver(III) complex of the *O*-confused oxaporphyrin derivative substituted at the tetrahedral C(3) positions by ethoxy and pyrrole moieties was also reported.[29]

The ability of carbaporphyrinoids to coordinate metal ions and to form metal−carbon bonds extends beyond the family of *N*- or *O*-confused porphyrins.[4,5,30−33] 6,11,16,21-Tetraphenylbenziporphyrin (TP*m*BP*H*)H gave organometallic complexes with palladium(II) and platinum(II), (TP*m*BP)Pd^{II} and (TP*m*BP)-Pt^{II}.[30] The metal ion is bound in the macrocyclic cavity by three pyrrolic nitrogens and a trigonal carbon of the benzene ring. A hydroxyl derivative of 8,9,13,14,18,19-hexaalkylbenziporphyrin, i.e., 8,19-dimethyl-9,13,14,18-tetraethyl-2-oxybenziporphyrin (OBP*H*)H_2,[34] coordinates palladium(II) to form the four-coordinate anionic complex $[(OBP)Pd^{II}]^-$ with the retention of macrocyclic aromaticity and coordination via a carbon σ-donor.[31] Subsequently, the palladium(II) complexes of core modified oxybenziporphyrin,[33] nickel(II), palladium(II) and platinum-(II) azuliporphyrins,[35,36] and silver(III) benzocarbaporphyrin were investigated.[37] 5,10,15,20-Tetraphenyl-*p*-benziporphyrin (TP*p*BPH_2)H − isomeric to 6,11,16,21-tetraphenyl-*m*-benziporphyrin − with the benzene ring linked at *para* positions formed a complex with cadmium(II) to reveal an unprecedented η^2 Cd(II)-arene interaction.[32]

Considering the coordination modes, established until now for carbacyclic fragments containing one carbon atom in the coordination core of carbaporphyrinoids, four fundamental types can be identified as represented here by monomeric *N*-confused porphyrin complexes (Chart 1).[4,5] The first one involves the replacement of the hydrogen atom by metal ions to yield a M−C σ-bond. The donor carbon atom is trigonally hybridized and metal ion is located in the porphyrin plane. Alternatively, the carbacyclic fragment is bound to metal via a pyramidal carbon in the η^1-fashion. The third mode, i.e., the side-on arrangement of the metal ion with respect to the planar carbacyclic moiety, preserves the basic structural features of the interacting ring including the trigonal sp^2 hybridization of the carbon center.[12,22,24,26,38]

Iron(II) inverted porphyrin complexes (*H*CTPP*H*)Fe^{II}Br **1** (Chart 2) and (*H*CTPP*H*)$Fe^{II}(SC_7H_7)$ present the conformation with the side-on position of the iron with respect to the inverted pyrrole plane.[25] The Fe···C(21) distances are longer than the regular iron−carbon bonds but shorter than the sum of van der Waals radii. The solid-state geometry of the Fe^{II}···{C(21)−H(21)} fragment in (*H*CTPP*H*)Fe^{II}Br and particularly the Fe···H(21) distance of 1.971 Å implied an agostic interaction.

Chart 1. Selected Coordination Modes of Monomeric 2-Aza-21-carbaporphyrin Complexes

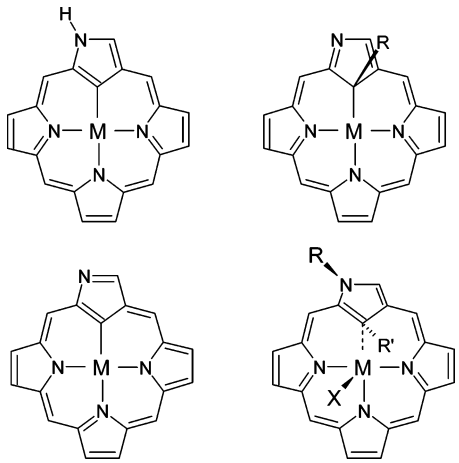

Chart 2. Iron(II) 2-Aza-5,10,15,20-tetraphenyl-21-carbaporphyrin

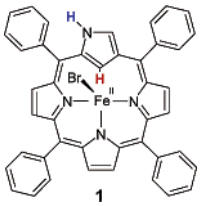

1

This uncommon type of a metal ion−inverted pyrrole ring interaction is reflected in ^{1}H NMR studies by an unprecedented isotropic shift (812 pm at 298 K) of the engaged H(21).[39] An agostic interaction has also been suggested for manganese *N*-inverted porphyrin complexes.[22] A dimeric iron(II) *N*-confused porphyrin, $[(CTPPH)Fe^{II}]_2$ was obtained from the anaerobic reaction of (*H*CTPP*H*)Fe^{II}Br with NaSePh. Under aerobic conditions, a μ-hydroxo bridged iron(III) dimer, $[(CTPPO)Fe^{III}]_2OH{\cdot}Na(THF)_2$, was obtained with Na^+ bridging the outer-N atoms. Oxygenation occurred at the inner core pyrrolic carbon to form a novel (CTPP*OH*)H_2 porphyrinic ring.[26]

The present contribution concerns with chemical oxidation and/or oxygenation of high-spin iron(II) complex (*H*CTPP*H*)-Fe^{II}Br **1**. Particular emphasis has been placed on ^{1}H and ^{2}H NMR studies as a source of insight into the electronic and molecular structure of these low symmetry iron(*n*) carbaporphyrinoids and as potential means for detecting intermediate species formed in the course of chemical processes. Their behavior with respect of iron−carbon bond reactivity can be compared to that of the related and much more intensively studied iron porphyrin and iron porphyrin aryl complexes,[40−42] which are of considerable interest in bioinorganic chemistry.

Results and Discussion

NMR Studies of Paramagnetic Iron(*n*) Complexes of 2-Aza-21-carbaporphyrin. The ^{1}H NMR data of paramagnetic

(29) Pawlicki, M.; Latos-Grażyński, L. *Chem.Eur. J.* **2003**, *9*, 4650.
(30) Stępień, M.; Latos-Grażyński, L. *Chem. Eur. J.* **2001**, *7*, 5113.
(31) Stępień, M.; Latos-Grażyński, L.; Lash, T. D.; Szterenberg, L. *Inorg. Chem.* **2001**, *40*, 6892−6900.
(32) Stępień, M.; Latos-Grażyński, L. *J. Am. Chem. Soc.* **2002**, *124*, 3838−3839.
(33) Venkatraman, S.; Anand, V. G.; Pushpan, S. K.; Sankar, J.; Chandrashekar, T. K. *Chem. Commun.* **2002**, 462.
(34) Lash, T. D. *Angew. Chem., Int. Ed. Engl.* **1995**, *34*, 2533.
(35) Graham, S. R.; Ferrence, G. M.; Lash, T. D. *Chem. Commun.* **2002**, 894.
(36) Lash, T. D.; Colby, D.; Graham, S. L.; Ferrence, G. M.; Szczepura, L. F. *Inorg. Chem.* **2003**, *42*, 7326.
(37) Muckey, M. A.; Szczepura, L. F.; Ferrence, G. M.; Lash, T. D. *Inorg. Chem.* **2002**, *41*, 4840.
(38) Furuta, H.; Ishizuka, T.; Osuka, A. *Inorg. Chem. Commun.* **2003**, *6*, 398.
(39) Rachlewicz, K.; Wang, S.-L.; Peng, C.-H.; Hung, C. H.; Latos-Grażyński, L. *Inorg. Chem.* **2003**, *42*, 7348.
(40) Arasasingham, R. D.; Balch, A. L.; Cornman, C. R.; Latos-Grażyński, L. *J. Am. Chem. Soc.* **1989**, *111*, 4357.
(41) Arasasingham, R. D.; Balch, A. L.; Hart, R. H.; Latos-Grażyński, L. *J. Am. Chem. Soc.* **1990**, *112*, 7566.
(42) Guilard, R.; van Caemelbecke, E.; Tabard, A.; Kadish, K. M. Synthesis, Spectroscopy and Electrochemical Properties of Porphyrins with Metal−Carbon; In *The Porphyrin Handbook*; Kadish, K. M., Smith, K. M., Guilard, R., Eds. Academic Press: San Diego, CA, 2000; pp 295−345.

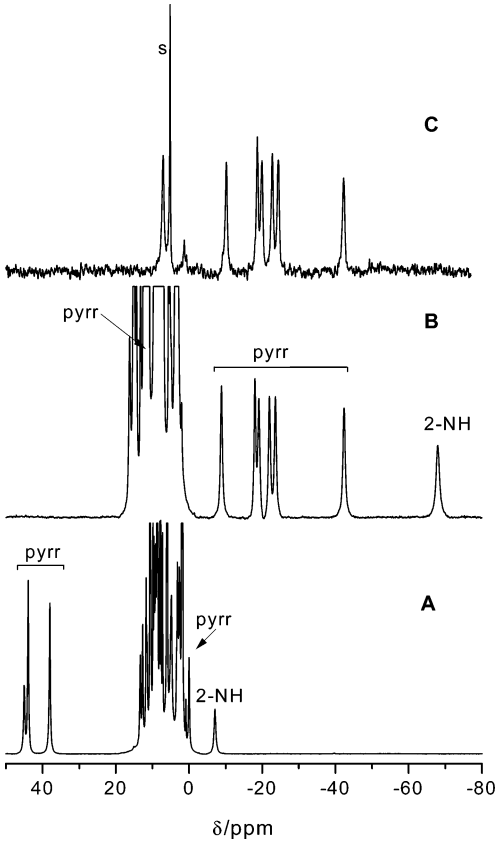

Figure 1. NMR spectra of iron inverted porphyrins: A, (*H*CTPP*H*)Fe^{II}Br **1** (^{1}H NMR, dichloromethane-d_2, 298 K); B, (*H*CTPP)Fe^{III}Br **2** (^{1}H NMR, dichloromethane-d_2, 298 K); C (*H*CTPP-d_7)Fe^{III}Br (^{2}H NMR, dichloromethane, 298 K).

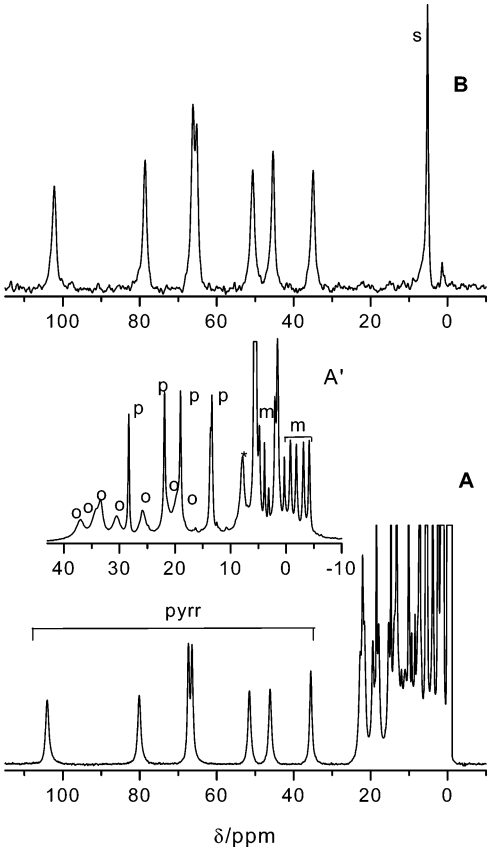

Figure 2. NMR spectra of **3**: A, [(CTPP*O*)Fe^{III}Br]$^-$ **3** (^{1}H NMR, dichloromethane-d_2, 298 K); B, [(CTPP*O*-d_7)Fe^{III}Br]$^-$ (^{2}H NMR, dichloromethane, 298 K). Inset A′ presents the *meso*-phenyl region (223 K). Peak labels in this and in following figures: pyrr−pyrrole resonances, o, m, p−resonances of ortho, meta, para hydrogens of *meso*-phenyl rings, * the decomposition product.

iron(n) inverted porphyrins (n = II,III), have been analyzed considering their C_1 symmetry as determined previously in the crystal structures of (*H*CTPP*H*)Fe^{II}Br **1**.[25] There are seven distinct β-H pyrrole positions for (*H*CTPP*H*)Fe^{II}Br **1**, a 2-NH position analogous to 2-CH of the regular porphyrin and four different meso sites. It may be anticipated that the ortho and meta positions on each *meso*-aryl ring will be distinguishable. Four para, eight ortho and eight meta resonances may therefore be expected for iron(n) 2-aza-5,10,15,20-tetraphenyl-21-carbaporphyrin complexes since the two opposite sides of the porphyrin are not equivalent. In the case of fast rotation, the number of ortho and meta resonances reduces to four each. On the other hand, four ortho, four meta and four para phenyl resonances are expected once two porphyrin sides are identical (e.g., six-coordinate complexes).

Respective ^{1}H and ^{2}H NMR spectra for (*H*CTPP*H*)Fe^{II}Br and its oxidation/oxygenation transformation products are presented in Figures 1−6. The spectral parameters have been gathered in Table 1. Resonance assignments, which are given above selected peaks, have been made on the basis of relative intensities, line widths, and site specific deuteration. As the spectroscopic analysis is primarily based on patterns of pyrrole resonances the ^{2}H NMR spectra of iron(n) inverted porphyrins are directly shown in each essential case. The plots of the temperature dependence of the chemical shifts which are typical for given electronic state of iron inverted porphyrin are shown in the Supporting Information (Figures 1S−5S)

Dioxygen Addition. Addition of dioxygen to dichloromethane−d_2 solution of (*H*CTPP*H*)Fe^{II}Br **1** produces marked changes in ^{1}H NMR spectra. The resonances of (*H*CTPP*H*)-Fe^{II}Br (Figure 1, Trace A) have decreased in intensity and new resonances, assigned to as (*H*CTPP)Fe^{III}Br **2**, have grown gradually (Figure 1, Trace B).

The total and selective conversion of **1** to **2** requires 12 h at 203 K but only 0.5 h at 298 K. In these experimental conditions we did not detected any intermediate, which could precede **2** in the reaction route. The spectral changes, similar to those shown in Figure 1, have also been detected when dioxygen is added to the solution of (*H*CTPP*H*)Fe^{II}Br in other solvents including chloroform-*d*, methanol-d_4, toluene-d_8, DMF-d_7, and DMSO-d_6. The pyrrole resonances of **2** are spread in the upfield 7.2 to −80.0 ppm region (298 K, dichloromethane-d_2). The most upfield located resonance at −76.6 ppm has been identified as corresponding to 2-NH position as is absent in ^{2}H NMR spectrum of (*H*CTPP-d_7)Fe^{III}Br but it is present in ^{1}H NMR of the same sample (Figure 1). The new species is stable in solution providing the dioxygen has been removed by freezing-thawing technique. Eventually, **2** has been isolated in the solid state and characterized by X-ray crystallography (see below).

The magnetic moment of (*H*CTPP)Fe^{III}Br **2** as measured by the Evans technique,[43] in a chloroform-*d* solution at 298 K equals 4.2 ± 0.1 μ_B. This value corresponds to the intermediate-spin state S = 3/2 of iron(III).[44−46] The signs and magnitudes

(43) Evans, D. F. J.; James, T. A. *J. Chem. Soc., Dalton Trans.* **1979**, 723.
(44) Evans, D. R.; Reed, C. R. *J. Am. Chem. Soc.* **2000**, *122*, 4660.

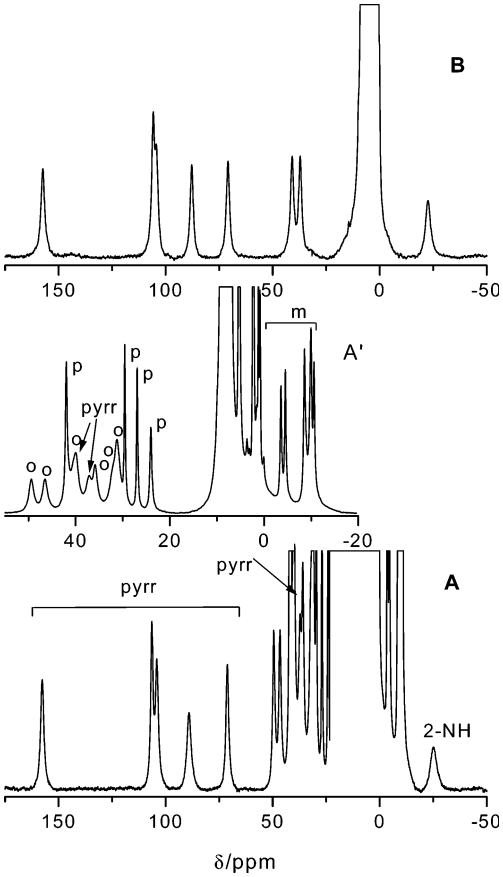

Figure 3. NMR spectra of: A, (*H*CTPP*O*)Fe^{III}Br **4** (^{1}H NMR, dichloromethane-d_2, 223 K); B, (*H*CTPP*O*-d_7)Fe^{III}Br (^{2}H NMR, dichloromethane, 223 K). Inset A′ presents the *meso*-phenyl region (223 K).

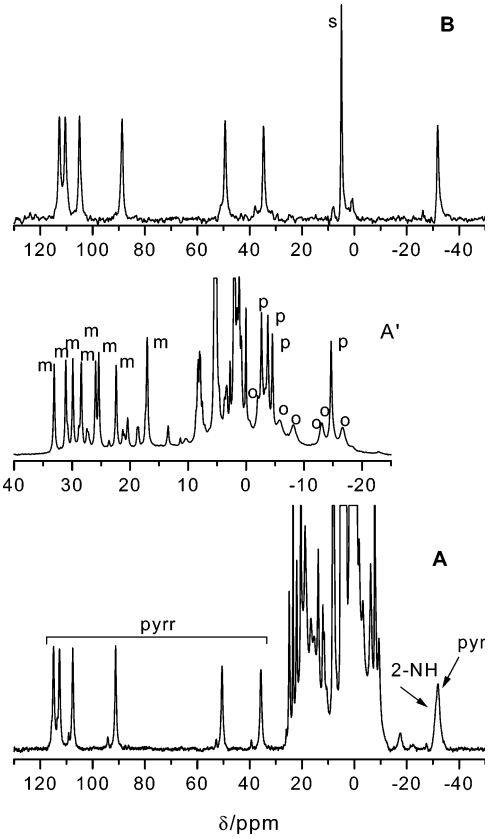

Figure 4. NMR spectra of iron(III) inverted porphyrin: A, [(*H*CTPP*H*)-Fe^{III}Br]$^+$ **5** (^{1}H NMR, dichloromethane-d_2, 298 K); B, [(*H*CTPP*D*-d_7)Fe^{III}-Br]$^+$ (^{2}H NMR, dichloromethane, 298 K). Inset A′ presents the *meso*-phenyl region (223 K).

of the isotropic shifts of **2** are consistent with such a ground electronic state as well. The value of $\mu = 4.9 \pm 0.1\ \mu_B$ has been determined for samples of high-spin iron(II) of (*H*CTPP*H*)-Fe^{II}Br **1**, which have been directly used to produce samples of **2** applied in magnetic moment measurements (see the Experimental section).

The subsequent changes in the ^{1}H NMR spectrum, caused by the permanent presence of dioxygen, have been followed systematically in the period of 12 h at 298 K. A set of seven downfield shifted pyrrole resonances, spread at the 110−30 ppm region (Figure 2), have been assigned to the high-spin derivative [(CTPP*O*)Fe^{III}Br]$^-$ **3**. The 2-NH resonance has not been detected. Compound **3** is formed by insertion of oxygen atom into the preformed Fe−C(21) bond of **2**. The magnetic moment of [(CTPP*O*)Fe^{III}Br]$^-$ **3** is $5.6 \pm 0.1\ \mu_B$ at 298 K. This value is typical of that of high-spin iron(III) porphyrins and it is consistent with ^{1}H NMR features of **3**.

The species **3** can be converted into the related high-spin derivative (*H*CTPP*O*)Fe^{III}Br **4** after addition of the acid (TFA) as shown in Figure 3. The species **4** presents the seven pyrrole resonances. The 2-NH resonance has been detected at low temperatures only (−25 ppm, 223 K). The protonation is reversible (e.g., an addition of collidine reverses the course of this reaction yielding **3**). The pattern and shift values resemble that of the conjugated base **3**, allowing the conclusion that the process involves the ligand protonation (vide infra) without changes of the ground electronic state of the metal ion. The final, stable product of oxygenation **4** was isolated and characterized by X-ray crystallography providing independent insight into the oxygenation/oxidation route (vide infra).

Reaction of (*H*CTPP*H*)Fe^{II}Br with Other Oxidizing Reagents. The anaerobic addition of 5 equiv. iodine to the solution of (*H*CTPP*H*)Fe^{II}Br **1** results exclusively in formation of [(*H*CTPP*H*)Fe^{III}Br]$^+$ **5** as confirmed by the distinct ^{1}H NMR spectrum (Figure 4).

Iodine reacts only as the one-electron oxidizing agent and the formed iodide anion does not enter the coordination sphere of the metal ion (as a sixth ligand or replacing the already coordinated bromide). Significantly, a titration of (*H*CTPP)-Fe^{III}Br **2** with trifluoroacetic acid, followed by ^{1}H NMR resulted in generation of [(*H*CTPP*H*)Fe^{III}Br]$^+$ **5** using an independent route according to eq 1

$$(H\text{CTPP})\text{Fe}^{III}\text{Br} + \text{H}^+ \leftrightarrows [(H\text{CTPP}H)\text{Fe}^{III}\text{Br}]^+ \qquad (1)$$

This process has a precedent. Previously the reversible protonation of the inner carbon of nickel(II) or copper(II) inverted porphyrin complexes was reported.[8,16] The pyrrole resonances of [(*H*CTPP*H*)Fe^{III}Br]$^+$ **5** are spread in the 100 to −40 ppm region reflecting the intrinsic asymmetry of the ligand and the high-spin state of the metal ion. The most upfield resonance has been identified as corresponding to 2-NH position as it absent in ^{2}H NMR spectrum of [(*H*CTPP*D*-d_7)Fe^{III}Br]$^+$ **5**, where

(45) Simonato, J.-P.; Pécaut, J.; Le Pape, L.; Oddou, J.-L.; Jeandey, C.; Shang, M.; Scheidt, W. R.; Wojaczyński, J.; Wołowiec, S.; Latos-Grażyński, L.; Marchon, J.-C. *Inorg. Chem.* **2000**, *39*, 3978.
(46) Rachlewicz, K.; Latos-Grażyński, L.; Vogel, E.; Ciunik, Z.; Jerzykiewicz, L. *Inorg. Chem.* **2002**, *41*, 1979.

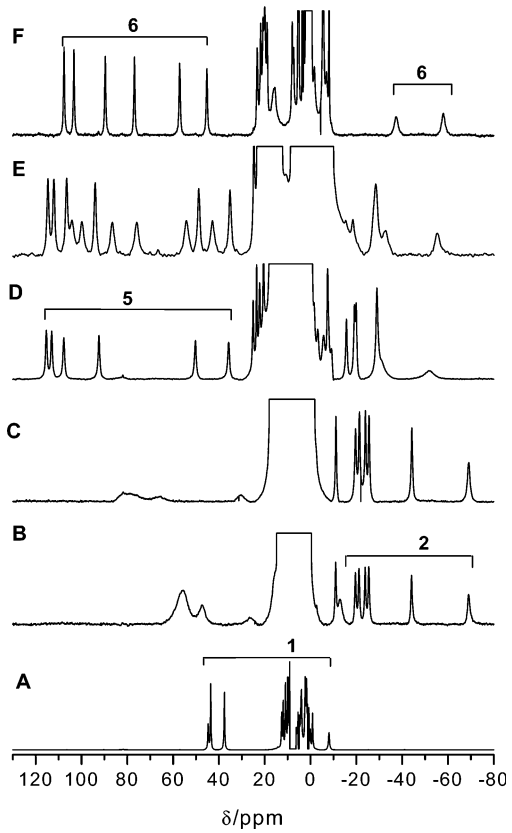

Figure 5. ^{1}H NMR spectra of [(*H*CTPP*H*)Fe^{II}Br] (dichloromethane-d_2, 298 K) after addition of Br_2: A, 0 equiv; B, 0.5 equiv; C, 0.7 equiv; D, 1. equiv; E, 1.5 equiv; F, 2 equiv. The peak labels refer to pyrrole resonances of dominating species as follows: B, [(*H*CTPP)Fe^{III}Br] **2**; D, [(*H*CTPP*H*)-Fe^{III}Br]$^+$ **5**, F, [(*H*CTPP*Br*)Fe^{III}Br]$^+$ **6**.

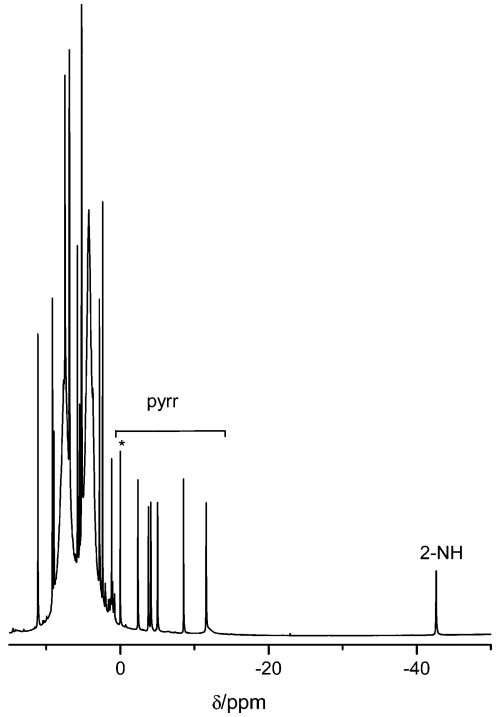

Figure 6. ^{1}H NMR spectrum of [(*H*CTPP)Fe^{III}(1-MeIm)$_2$]$^+$ **7** (dichloromethane-d_2, 298 K, 10 equiv of 1-MeIm added). The solvent impurity in region of pyrrole resonances marked with *.

the ligand is deuterated in all pyrrolic positions, but it was present in ^{1}H NMR collected for [(*H*CTPP*H*)Fe^{III}Br]$^+$. Presumably, the accompanying upfield resonance belongs to the same pyrrole (3-H) as the peculiar upfield position of these resonances may reflect the specific location of the inverted pyrrole with respect to the metal ion.[12] An effort has been made to locate the H(21) resonance of [(*H*CTPP*H*)Fe^{III}Br]$^+$ in ^{1}H NMR or D(21) of [(*H*CTPP*D*-d_7)Fe^{III}Br]$^+$ in ^{2}H NMR similarly as it has been done for the iron(II) derivative.[39] The substantially larger broadening of all perimeter β-H pyrrole resonances has been seen for [(*H*CTPP*H*)Fe^{III}Br]$^+$ **5** in comparison to (*H*CTPP*H*)-Fe^{II}Br **1**. Presuming that the similar relation of line width due to the analogous structures and mechanisms of spin delocalization holds for the H(21) position for [(*H*CTPP*H*)Fe^{III}Br]$^+$ **5** and (*H*CTPP*H*)Fe^{II}Br **1** the predicted line width of H(21) is well in excess of reasonably observed lines in the conditions of our experiment.

A careful titration of (*H*CTPP*H*)Fe^{II}Br **1** with Br_2 has been carried out in strictly anaerobic conditions. The effect of addition of less than 1 equiv of bromine to a solution of (*H*CTPP*H*)-Fe^{II}Br is shown in the ^{1}H NMR spectrum (Trace B of Figure 5). Separate resonances of (*H*CTPP)Fe^{III}Br **2**, assigned previously once dioxygen reacted with **1**, are readily detected (Figure 5, Traces B and C). Simultaneous broadening of (*H*CTPP*H*)-Fe^{II}Br **1** resonances and their gradual relocation in the course of titration have also been noticed. Eventually, the originally broadened lines resembling the spectrum of (*H*CTPP*H*)Fe^{II}Br transform into the characteristic set of resonances assigned to [(*H*CTPP*H*)Fe^{III}Br]$^+$ **5**, (Figure 5, Trace D), i.e., to the product of one-electron, metal-centered oxidation of (*H*CTPP*H*)Fe^{II}Br **1**. Thus, in the course of this one-electron oxidation two iron-(III) products **2** an **5** have been formed as accounted for by the ^{1}H NMR spectrum (Figure 5, Traces C and D). Separate resonances of (*H*CTPP*H*)Fe^{II}Br **1** and [(*H*CTPP*H*)Fe^{III}Br]$^+$ **5** could not be detected in the course of titration with bromine. Instead, an averaged pattern has been observed. Thus, the rate of electron exchange between these two species is fast on the ^{1}H NMR time scale suggesting that relatively modest structural changes occur in the course of the redox process. Addition of further portions of the titrant to the solution containing (*H*CTPP)Fe^{III}Br and [(*H*CTPP*H*)Fe^{III}Br]$^+$ produces the spectrum shown in Trace F of Figure 5. At this stage, resonances of **2** and **5** diminished to the point where they are no longer observed but the resonances of the new compound **6** have grown. The ^{1}H NMR patterns of **5** and **6** are consistent with the high-spin ground electronic state. The multiplicity of *meso*-phenyl resonances of **5** and **6** reflects the unequivalency of two carbaporphyrins sides due to a five-coordination and side-on arrangement of the inverted pyrrole fragments. The species **6** has also been formed once the strongly oxidizing reagent phenoxatine hexachloroantimonate reacted with (*H*CTPP*H*)Fe^{II}Br **1** (anaerobic conditions) or (*H*CTPP)Fe^{III}Br **2** (aerobic conditions). In these experimental conditions, [(*H*CTPP*H*)Fe^{III}Br]$^+$ **5** undergoes substitution at C(21) to form [(*H*CTPP*Br*)Fe^{III}Br]$^+$ **6**. This substitution has been confirmed by mass spectrometry. The mass spectra has been measured directly for the sample of **6** obtained in the ^{1}H NMR course of titration with Br_2. In the conditions of our experiment (ES), the most intense peak m/z = 694.5 corresponds to the demetalation product of **6**, i.e., -(*H*CTPP*Br*)-H_2. Previously, it was documented that the C(21) atom of inverted porphyrin are susceptible to substitution reactions.

Table 1. ^{1}H NMR Chemical Shifts of Iron(II) of 2-Aza-21-carbaporphyrin and Its Oxidation and Oxygenation Product

compound		chemical shifts[a] pyrrole	2-NH
(*H*CTPP*H*)Fe^{II}Br	**1**	44.8, 43.7, 43.7, 31.7, 31,7, 8.4, 0.78	−8.0
(*H*CTPP)Fe^{III}Br	**2**	7.2, −10.6, −19.2, −20.6, −23.2, −24.9, −43,2	−76.6
[(CTPP*O*)Fe^{III}Br]$^-$	**3**	106.3, 82.2, 69.4, 68.5, 53.5, 48.1, 37.5	
[(*H*CTPP*O*)Fe^{III}Br	**4**	117.3, 80.0, 76.8, 69.1, 59,1, 31,3, 29.3	−25.0[b]
[(*H*CTPP*H*)Fe^{III}Br]$^+$	**5**	115.2, 112.9, 107.9, 91.5, 50.7, 35.9, −32.8	−31.2
[(*H*CTPP*Br*)Fe^{III}Br]$^+$	**6**	108.7, 104.4, 90.5, 76.9, 58.0, 46.1, −58.6	−39.7
[(*H*CTPP)Fe^{III}(1-MeIm)]$_2^+$	**7**	1.3, −2.3, −3.7, −4.1, −4.95, −8.5, −11.5	−42.6

[a] δ/ppm, at 298 K unless marked differently. [b] at 223 K, all measurements in dichloromethane-d_2.

Examples reported to date include alkylation,[7,10,12,47] halogenation,[48,49] nitration,[50] or cyanation.[51]

As described above, the reaction of (*H*CTPP*H*)Fe^{II}Br **1** with dioxygen ends up with formation of [(CTPPO)Fe^{III}Br]$^-$ **3**. Significantly, we have found that the conversion of [(*H*CTPP-*Br*)Fe^{III}*Br*]$^+$ **6** into [(CTPPO)Fe^{III}Br]$^-$ **3** has taken place, presumably by nucleophilic substitution featuring water as nucleophile, once the ^{1}H NMR sample of [(*H*CTPP*Br*)Fe^{III}Br]$^+$ **6** was kept in dichloromethane-d_2 saturated with D_2O.

Titration of (*H*CTPP)Fe^{III}Br with 1-MeIm. Coordination of nitrogen base has been of interest because of possible correlations between the ground electronic state, coordination mode and ^{1}H NMR spectroscopic patterns of iron(*n*) carbaporphyrins.

Addition of 1-methylimidazole to a solution of (*H*CTPP)-Fe^{III}Br **2** in dichloromethane results in its conversion to a six-coordinate low-spin complex [(*H*CTPP)Fe^{III}(1-MeIm)$_2$]$^+$ **7**. The representative ^{1}H NMR spectrum is shown in Figure 6. The characteristic set of eight upfield shifted resonances (β-H, 2-NH, and 3-H) of **2** spread at the 7.2 to −76.6 region, have been replaced by an analogous set assigned to [(*H*CTPP)Fe^{III}-(1-MeIm)$_2$]$^+$ **7** which demonstrate markedly smaller paramagnetic shifts. These resonances are accompanied by sets of upfield shifted ortho and para meso phenyl proton resonances and downfield shifted meta protons. The observation of 1-MeIm resonances and their relative intensity with respect to β-H resonances presents convincing evidence for the presence of two axial ligands. In general the spectroscopic data are consistent with the low-spin ground electronic state of [(*H*CTPP)Fe^{III}(1-MeIm)$_2$]$^+$.[52]

X-ray Structures of (*H*CTPP)Fe^{III}Br 2 and (*H*CTPP*O*)-Fe^{III}Br 4. Once the conditions were determined, an attempt was made to crystallize some of the species detected by ^{1}H NMR spectroscopy. The respective structures and essential structural parameters are shown at Figures 7−10 and in Table 2. In each case the identity of the crystallized compound has been confirmed by the ^{1}H NMR spectroscopy to eliminate a possibility of any substantial chemical changes in the course of crystallization.

Compound **2** crystallized in the monoclinic space group $P2_1/n$ with four molecules in the unit cell. The crystal structure of

Table 2. Selected Bond Lengths (Å) and Angles (deg) for (*H*CTPP)Fe^{III}Br **2** and (*H*CTPP*O*)Fe^{III}Br **4**

	2	**4**
Fe−Br1	2.443(2)	2.3906(12)
Fe−N22	1.985(8)	2.104(5)
Fe−N23	2.045(7)	2.046(5)
Fe−N24	2.023(8)	2.102(5)
Fe−C21	1.981(8)	2.192(6)
Fe−O1		2.041(5)
O1−C21		1.299(7)
C1−C21	1.435(1)	1.470(9)
C4−C21	1.393(1)	1.463(9)
C1−N2	1.407(11)	1.401(8)
N2−C3	1.341(11)	1.311(8)
C3−C4	1.421(11)	1.393(8)
C4−C5	1.420(12)	1.374(8)
C1−C20	1.376(13)	1.400(9)
Br1−Fe−C21	100.0(2)	94.62 (19)
Fe−O1−C21		78.6(4)
O1−C21−Fe		65.9(3)
C1−N2−C3	110.7(9)	108.7(6)
N2−C3−C4	107.4(1)	113.7(6)
C3−C4−C21	109.1(9)	105.1(6)
C4−C21−C1	106.3(8)	104.7(6)
C21−C1−N2	106.5(1)	107.3(6)

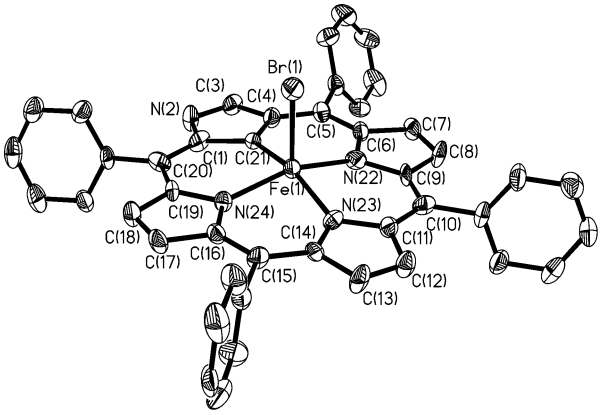

Figure 7. Perspective drawing (with 35% probability ellipsoid) of (*H*CTPP)Fe^{III}Br **2**.

(*H*CTPP)Fe^{III}Br **2** has a planar porphyrin ring (Figure 7). The averaged deviation of 24 core-atoms from a plane defined by three pyrrolic nitrogens and the inner core carbon is 0.077 Å. The iron sits 0.336 Å above the plane. A non bonded contact with distance of 2.822 Å between axial bromide and peripheral N−H of the neighboring carbaporphyrin ring agrees with the assignments of atoms on the inverted pyrrole ring. Consequently, the shortest distance of 1.981(8) Å among the four bonds of iron and inner coordination sphere atoms has been assigned as Fe−C bond. Nevertheless, the distance of 1.981(8) Å for Fe−C bond in **2** is comparable to 1.955(3) Å for the Fe−C distance of low-spin five-coordinate phenyl(*meso*-tetraphenylporphyri-

(47) Schmidt, I.; Chmielewski, P. J. *Chem. Commun.* **2002**, 92.
(48) Furuta, H.; Ishizuka, T.; Osuka, A.; Ogawa, T. *J. Am. Chem. Soc.* **1999**, *121*, 2945.
(49) Furuta, H.; Ishizuka, T.; Osuka, A.; Ogawa, T. *J. Am. Chem. Soc.* **2000**, *122*, 5748.
(50) Ishikawa, Y.; Yoshida, I.; Akaiwa, K.; Koguchi, E.; Sasaki, T.; Furuta, H. *Chem. Lett.* **1997**, 453.
(51) Xiao, Z.; Patrick, B. O.; Dolphin, D. *Chem. Commun.* **2003**, 1062.
(52) Walker, F. A. Proton NMR and EPR Spectroscopy of Paramagnetic Metalloporphyrins; In *The Porphyrin Handbook*; Kadish, K. M., Smith, K. M., Guilard, R., Eds. Academic Press: San Diego, CA, 2000; pp 81−183.

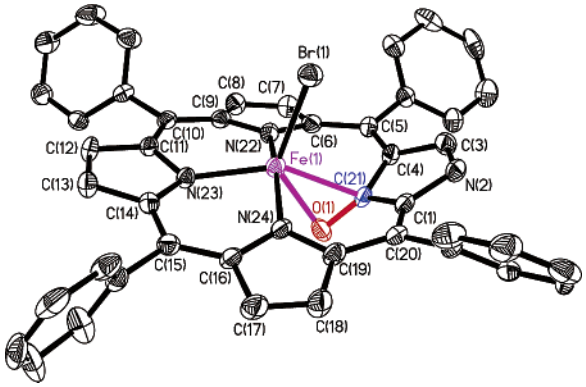

Figure 8. Perspective drawing (with 35% probability ellipsoid) of (*H*CTPP*O*)Fe^{III}Br **4**.

nato)iron(III).[53] The applicable Fe−C(pyrrole) bond distance equals 1.962(2) Å as determined for the dinuclear compound produced in reaction of Fe_2CO_9 with heterocyclic imines and *N*-methyl-pyrrole carbaldehyde [μ_2-η^3-$CH_3N{-}CH_2{-}C{=}CH{-}CH{=}CH{-}NCH_3$]$Fe_2(CO)_6$ but the pyrrolic ring is also involved in interaction with the adjacent Fe(CO_3) unit.[54,55] The averaged bond distance of 2.018(8) Å for the three Fe−N_p bonds in **2** is shorter than corresponding averaged distance 2.096(8) Å for (*H*CTPP*H*)Fe^{II}Br **1**.[25] Interestingly, the average Fe−N_p distance in **2** is shorter than 2.070 Å Fe−N bond lengths of iron(III) porphyrin complexes with high-spin electronic state but is comparable to Fe−N_p bond lengths of intermediate-spin iron(III) porphyrins 1.997 Å.[45,56]

The structure of **4** determined in an X-ray diffraction study is shown in Figure 8.

The crystal structure of **4** has a monoclinic space group *C*2/*c* with eight molecules in the unit cell. The peripheral nitrogen and carbon on the inverted pyrrole ring were refined as mutually disordered. Identical coordinates and thermal-parameters were used for the refinements of overlapping carbon and nitrogen. The carbaporphyrin ring of **4** exhibits a nonplanar geometry with the inverted pyrrole ring tilted away from the porphyrin plane which resembles the geometry of (*H*CTPP*H*)Fe^{II}Br **1**.[25] The torsion angles between the inverted pyrrole ring and neighboring pyrrole rings are 31.8° (N22) and 28.2° (N24). The porphyrin core as a whole exhibits saddle shape distortion with a mean deviation of 0.226 Å from the plane defined by three pyrrolic nitrogens. The alternate sign of deviations of the neighboring pyrrole rings are consistent with the saddle distortion (Figure 9).

The iron lies 0.309 Å above the N_3 plane. An oxygen atom is inserted into the Fe−C bond and is nearly coplanar to the inverted pyrrole ring with deviations of 0.411 and 0.272 Å from the averaged inverted pyrrole plane and the plane defined by C1, C21, and C4, respectively.

Interestingly, the distances and angles surrounding inverted pyrrole ring and oxygen for **4** can be compared to the dimeric complex, [(CTPP*O*)Fe^{III}]$_2$OH·Na(THF)$_2$. The comparison suggest the preference for different tautomers of the equatorial

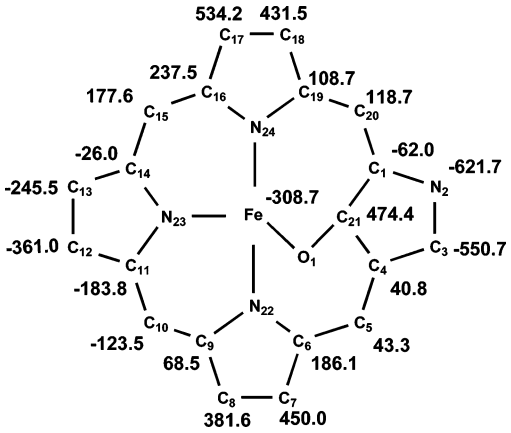

Figure 9. The deviations of atoms (in 0.001 Å) from the mean-plane defined by three coordination sphere pyrrolic nitrogens of (*H*CTPP*O*)Fe^{III}-Br **4**.

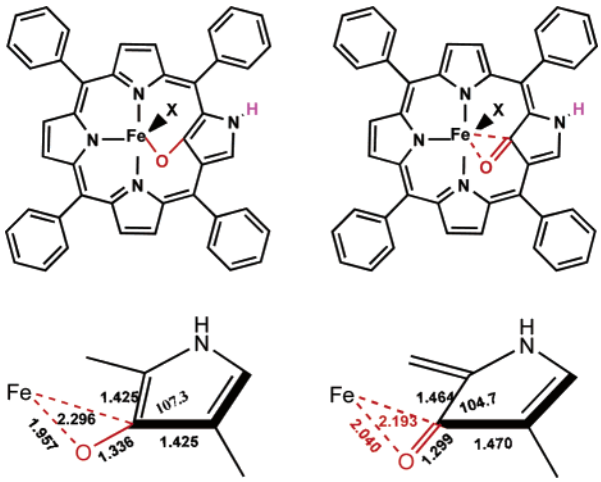

Figure 10. Comparison of coordination modes of [(CTPP*O*Fe^{III})]$_2$OH·Na(THF)$_2$ (left) and (HCTPP*O*)Fe^{III}Br **4**. (right).

ligand in these two complexes.[26] As depicted in Figure 10, the C=O distance of 1.299(7) Å in **4** is shorter than 1.336(5) Å found in the dimeric complex and closer to C=O distances for dioxoporphodimethane type complexes 1.223(6).[57,58] The C−O distance 1.336(5) Å is typical of phenoxide ligands,[59] and pyrrolic alkoxide fragment (1.300−1.360 Å) of cyclic iron(III) trimer.[60] The bond distances from inner carbon to neighboring pyrrolic carbons (C(21)−C(1) and C(21)−C(4) of 1.470(9) and 1.463(9) Å in **4** are both longer than corresponding distances in the dimeric [(CTPP*O*)Fe^{III}]$_2$OH·Na(THF)$_2$ complex which is consistent with a keto-like structure. The IR measurements have been carried out for the solid sample of **4**. A stretching CO band appeared at 1706.4 cm^{-1}, which confirmed the presence of carbonyl group.

Moreover, the Fe−C(21) distance of 2.199(7) Å for **4** is significantly shorter than 2.296(5) Å detected for [(CTPP*O*)-Fe^{III}]$_2$OH·Na(THF)$_2$.[26] The Fe−O(1) distance 2.041(5) Å is significantly longer that the Fe−O distances (1.873−1.886 Å) found for cyclic iron(III) 2-hydroxyporphyrin trimer where the pyrrolic alkoxide coordination was described.[60] Thus, a direct

(53) Dopplet, P. *Inorg. Chem.* **1984**, *23*, 4009.
(54) Imhof, W. *J. Organomet. Chem.* **1997**, *533*, 31.
(55) Imhof, W. *J. Organomet. Chem.* **1997**, *541*, 109.
(56) Scheidt, W. R.; Gouterman, M. In *Iron Porphyrin, Part I.*; Lever, A. B. P., Gray, H. B., Eds.; Addison-Wesley, Inc.: Reeding, 2003; pp 111−122.
(57) Senge, M. O.; Smith, K. M. *Z. Naturforsch.* **1992**, *47*, 837.
(58) Balch, A. L.; Olmstead, M. M.; Phillips, S. L. *Inorg. Chem.* **1993**, *32*, 3931.
(59) Stępień, M.; Latos-Grażyński, L. *Inorg. Chem.* **2003**, *42*, 6183.
(60) Wojaczyński, J.; Latos-Grażyński, L.; Olmstead, M. M.; Balch, A. L. *Inorg. Chem.* **1997**, *36*, 4548.

Scheme 1. Oxidation of (*H*CTPP*H*)Fe^{II}Br

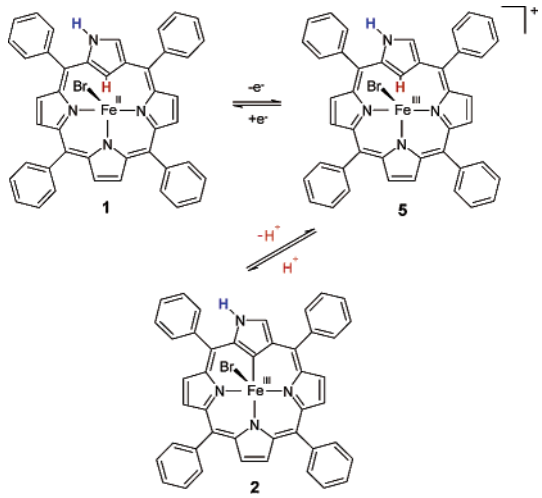

Scheme 2. Substitution

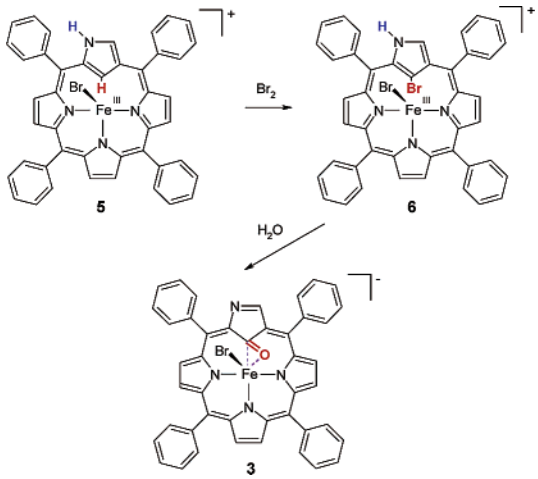

interaction between the iron center and the π electron density on the C(21)═O carbonyl group is evident. The projection of the iron(III) ion onto the C(21)−O bond lies close to its center as readily reflected by the appropriate angles Fe−C(21)−O 65.9(3)° and Fe−O−C(21) 78.6(4)°. Thus, the metal ion interacts with the C═O fragment in a η^2 fashion. Recently, such a coordination mode was reported by Dolphin and co-workers for nickel(III) complex *N*-confused porphyrin inner C-oxide.[15]

Noticeably, the angles between phenyl rings and porphyrin core are significantly affected by the geometry of pyrrole rings. The phenyl rings neighboring to tilted inverted pyrrole ring give dihedral angles of 42.1(2) and 43.4(3)° to the plane defined by three internal pyrrolic nitrogens. These dihedral angles are smaller than 64.3(2) and 51.0(2)° for two phenyl rings inside the tripyrrolic unit of the carbaporphyrin core.

Oxidation/Oxygenation Mechanisms. The NMR study accompanied by crystallographic data demonstrates that (*H*CTPP*H*)Fe^{II}Br undergoes oxidation and oxygenation which result a series of paramagnetic complexes. These species are most readily detected by ^{1}H NMR spectroscopy. To account for the detected ^{1}H NMR spectroscopic pattern in the presence of dioxygen we have considered the following phenomena: one electron oxidation of (*H*CTPP*H*)Fe^{II}Br **1** to form [(*H*CTPP*H*)-Fe^{III}Br]$^+$ **5**, protonation/deprotonation at the C(21) carbon atom, and oxygenation at the C(21) carbon atom to produce the CO fragment, which coordinates to the iron(III) central ion. In addition, changes of the unpaired spin density distribution due to the axial ligation and protonation of N(2) nitrogen atom have been considered. Finally, we have detected that the substitution of the H(21) with the bromine atom plays an essential role once dibromine has been applied in excess as the oxidizing agent.

The process of one-electron oxidation is likely to proceed as shown in Scheme 1. Depending on the choice of oxidizing agent a preference for **5** (I_2) or **2** (O_2) has been observed. Only in the course of oxidation with Br_2 two iron(III) inverted porphyrin complexes (**2** and **5**) remained in the detected acid−base equilibrium in the presence of iron(II) complex. Once formed the species **2** can be converted into **5** by addition of acid.

Addition of Br_2 to the solution containing [(*H*CTPP)Fe^{III}Br] **2** and [(*H*CTPP*H*)Fe^{III}Br]$^+$ **5** results in bromination at C(21) yielding [(*H*CTPP*Br*)Fe^{III}Br]$^+$ **6** in accord with typical inverted porphyrin reactivity.[7] The subsequent reaction with water results finally in formation of the C═O fragment (Scheme 2). Analogously, the reaction of benzocarbaporphyrin with aqueous ferric chloride (ferric bromide) afforded in a regioselective process the corresponding 21-chlorobenzocarbaporphyrin (21-bromobenzocarbaporphyrin).[61] The species **3** and its conjugated acid **4** contain a ligand which is an 2-aza-21-carbaporphyrin derivative with the oxygen atom located on the inner carbon−*N*-confused porphyrin C-oxide. Originally, such a ligand has been detected in the dimeric product of [(CTPP*H*)Fe^{II}]$_2$ oxygenation although in different tautomeric form,[26] and in oxidation of (*H*CTPP)-Ni^{II} with OsO_4.[15] In this work, the species **3** and **4** have been generated in the course of oxygenation of **2** as discussed below.

In the course of our NMR and X-ray studies on oxidation and oxygenation of iron(II) 2-aza-21-carbaporphyrin we have trapped two essential steps of the process (Scheme 3). The formation of **2** requires a one-electron oxidation. In the case where dioxygen is the oxidant the formation of a superoxide is implied.[41] One electron oxidation is accompanied by deprotonation of C(21)−H and resembles the process shown in Scheme 1. The next step requires an insertion of the oxygen atom into the Fe^{III}−C bond to obtain **3** and eventually its conjugated acid **4**. The coordination of iron(III) favors the resonance structure **4***A*, where the carbaporphyrinoids acts as a trianionic ligand. Thus, in absence of some acid in excess the 2-NH proton of **4** dissociates readily to form **3**.

As matter of fact the reaction of **2** to produce **4** resembles the reaction of dioxygen with low-spin, five-coordinate complexes, (P)Fe^{III}Ar (P, porphyrin dianion; Ar, aryl group) which produced (P)Fe^{III}OAr.[41] Thus, for oxygenation of **2** one can consider a course of the reaction (Scheme 4), which involves an initial insertion of dioxygen into the Fe−C bond to form a transient form **T**-*1* (alternatively the four-center transition state **T**-*1′* can be considered). The peroxide intermediate is expected to be extremely short-lived. Thus, the insertion step should be followed by rapid homo- or heterolysis of the peroxide moiety. Only the heterolytic route leading to **T**-*2* has been shown in Scheme 4. Thus two reactive centers, which are locked in the cage created by the restrains of macrocycle, are generated. The CO fragment coordinates to the metal ion. The reaction with the surrounding solvents converts highly oxidized iron center into iron(III). Likely, the oxygen atom is transferred to solvent

(61) Lash, T. D.; Muckey, M. A.; Hayes, M. J.; Liu, D.; Spence, J. D.; Ferrence, G. M. *J. Org. Chem.* **2003**, *68*, 8558.

Scheme 3. Oxygenation

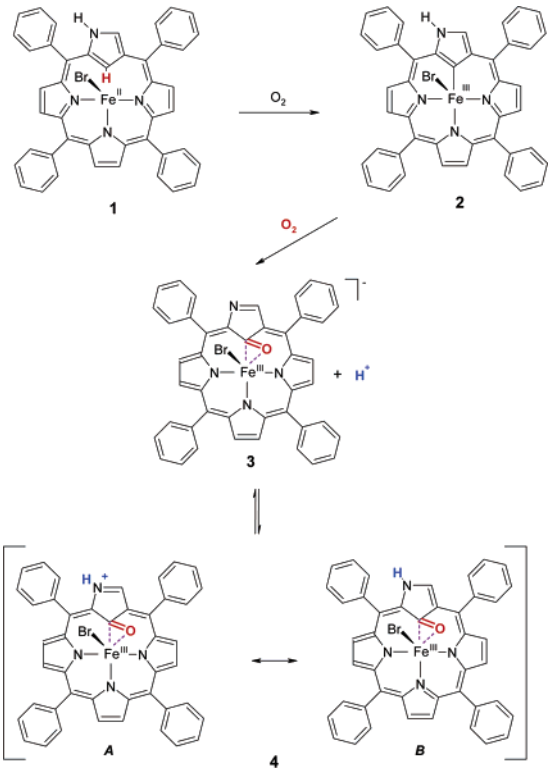

Scheme 4. Suggested Oxygenation Mechanism

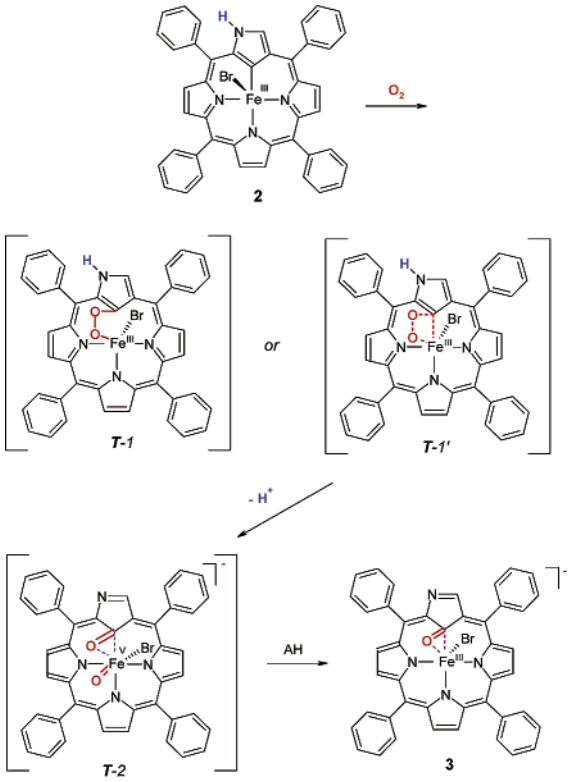

molecules.[62−64] Altogether the macrocycle gains an oxo functionality in its coordination core. Actually the addition of *m*-CPBA, a typical donor of an oxygen atom, to the solution of (*H*CTPP)Fe^{III}Br **2** affords **4** as well. In our opinion, there is a significant parallel between the reaction of **2** with *m*-CPBA to yield **4** and the reaction of (TMP)Fe^{III}Cl with *m*-CPBA to produce iron(III) porphyrin *N*-oxide.[65−68]

Electronic Structure of Iron(*n*) Inverted Porphyrins−^{1}H NMR Studies. Generally, ^{1}H NMR spectroscopy was shown to be a definitive method for detecting and characterizing iron(*n*) porphyrins (n = I−IV),[52] and lower symmetry derivatives modified at the coordination core: iron(*n*) *N*-substituted porphyrins (n = II−IV),[52,69−73] iron(II) 21-thiaporphyrin,[74] and iron(*n*) 21-oxaporphyrin (n = I−III).[75] The hyperfine shift patterns, that were recorded for iron porphyrins[52,76] are sensitive to the iron oxidation, spin and ligation states. The intermediate iron porphyrins, acting in dioxygen activation of oxygen atom transfer, have been trapped by NMR spectroscopy.[40,77−79] The fundamental spectroscopic features have been preserved in iron complexes of core modified porphyrins (N−CH$_3$, O, S, N−C−Fe) providing that spin/electronic state are identical.[52,69−75,80]

The ^{1}H NMR spectra of iron(*n*) inverted porphyrins display characteristics that clearly reveal the lowering of symmetry. Thus, the spread of regular β-H resonances are markedly larger than for more symmetrical counterparts. Nevertheless, the pattern of chemical shifts for these iron(III) inverted porphyrins resembles that of iron(*n*) porphyrins and of core modified iron(*n*) porphyrins. An average chemical shift of the perimeter resonances as determined at 298 K has been considered here as a suitable parameter to characterize the ground electronic/spin state of iron(*n*) inverted porphyrins. Thus the average shifts for six regular pyrroles have been examined for **1**, **5**, and **6** where a side-on location of the metal ion with respect to the *N*-confused pyrrole ring has been determined**.** The chemical shift values of all downfield resonances for **3** and **4** have been included to calculate the arithmetic mean. In two cases: **7** and **2**, where all internal donors including the C(21) atom are involved in regular coordination, the shifts of eight upfield resonances including 2-NH contributed to the average. These values decrease in a series **5**, 85.3 (79.3); **6**, 80.8 (62.6); **4**, 66.1 (87.7); **3**, 64.4 (68.5); **1**, 24.1 (52.8); **7**, −9.5 (43.9); **2**, −26.4 (83.8) (in ppm at 298 K, in parentheses the spread of chemical shifts included in mean values are given). Actually, the average shift values of **3**, **4**, **5**, and **6** approach those found for high-spin iron(III) tetraarylpor-

(62) Gold, A.; Joyaray, K.; Doppelt, P.; Weis, R.; Chottard, G.; Bill, E.; Ding, X.; Trautwein, A. X. *J. Am. Chem. Soc.* **1988**, *110*, 5756.
(63) Mizutani, Y.; Hashimoto, S.; Tatsuno, Y.; Kitagawa, T. *J. Am. Chem. Soc.* **1990**, *112*, 6809.
(64) Groves, J. T.; Gross, Z.; Stern, M. K. *Inorg. Chem.* **1994**, *33*, 5065.
(65) Groves, J. T.; Watanabe, Y. *J. Am. Chem. Soc.* **1988**, *110*, 8443.
(66) Tsurumaki, H.; Watanabe, Y.; Morishima, I. *J. Am. Chem. Soc.* **1993**, *115*, 11 784.
(67) Latos-Grażyński, L.; Cheng, R.-J.; La Mar, G. N.; Balch, A. L. *J. Am. Chem. Soc.* **1981**, *103*, 4270.
(68) Rachlewicz, K.; Latos-Grażyński, L. *Inorg. Chem.* **1996**, *35*, 1136.
(69) Balch, A. L.; Chan, Y.-W.; La Mar, G. N.; Latos-Grażyński, L.; Renner, M. W. *Inorg. Chem.* **1985**, *24*, 1437.
(70) Balch, A. L.; La Mar, G. N.; Latos-Grażyński, L.; Renner, M. W. *Inorg. Chem.* **1985**, *24*, 2432.
(71) Wysłouch, A.; Latos-Grażyński, L.; Grzeszczuk, M.; Drabent, K.; Bartczak, T. *J. Chem. Soc., Chem. Commun.* **1988**, 1377.
(72) Balch, A. L.; Cornman, C. R.; Latos-Grażyński, L.; Olmstead, M. M. *J. Am. Chem. Soc.* **1990**, *112*, 7552.
(73) Balch, A. L.; Cornman, C. R.; Latos-Grażyński, L.; Renner, M. W. *J. Am. Chem. Soc.* **1992**, *114*, 2230.
(74) Latos-Grażyński, L.; Lisowski, J.; Olmstead, M. M.; Balch, A. L. *Inorg. Chem.* **1989**, *28*, 1183.
(75) Pawlicki, M.; Latos-Grażyński, L. *Inorg. Chem.* **2002**, *41*, 5866.
(76) Bertini, I.; Luchinat, C. *Coord. Chem. Rev.* **1996**, *150*, 1.
(77) Balch, A. L.; Latos-Grażyński, L.; Renner, M. W. *J. Am. Chem. Soc.* **1985**, *107*, 2983.
(78) Balch, A. L.; Chan, Y.-W.; Cheng, R.-J.; La Mar, G. N.; Latos-Grażyński, L.; Renner, M. W. *J. Am. Chem. Soc.* **1984**, *106*, 7779.
(79) Rachlewicz, K.; Latos-Grażyński, L.; Vogel, E. *Inorg. Chem.* **2000**, *39*, 3247.

phyrins,[52] iron(III) β-substituted tetraarylporphyrin[81] and iron(III) *N*-methyltetraarylporphyrin (the average value for regular pyrrole rings).[70] The average chemical shift of **1** is consistent with that found for high-spin iron(II) tetraarylporphyrins, iron(II) *N*-methyltetraarylporphyrin, and iron(II) 21-thia-tetraarylporphyrin.[52,69,74] Finally, the upfield positions, seen for **2** and **7**, are clearly consistent with the intermediate- and low-spin states respectively considering the asymmetric iron(III) porphyrins as the reference molecules.[45,46,52,72,80]

In the high-spin ion(III) complexes **5** and **6** the distinct low field positions of β-H resonances assigned to the regular pyrroles accompanied by the sign alternations detected for *ortho*-H, *meta*-H, *para*-H of *meso*-aryls respectively provide an evidence for the domination of contact contribution in isotropic shifts. Thus the paramagnetic shifts of **5** and **6** can be explained by a model typically applied to regular iron porphyrins and iron *N*-substituted porphyrins. In the case of a high-spin iron(III) center—$(d_{xy})^1(d_{xz})^1(d_{yz})^1(d_{z^2})^1(d_{x^2-y^2})^1$—both σ and π routes of spin density delocalization operate.[52,81,82] Typical delocalization pathways involve delocalization through a σ-framework by way of σ-donation to the half occupied $(d_{x^2-y^2})^1$ iron(III) orbital. Additionally the π-delocalization locates a considerable amount of spin density at β-C, β-H, and *meso* positions.[41,52,70,72,75,81] Actually the variation of the β-H positions in the ^{1}H NMR spectrum may be accounted for by specific π-delocalization mechanisms.[81,82]

In principle, the β-H isotropic shifts of **3** could be explained by the similar spin delocalization mechanism as described for **5** and **6**. However, once the oxygen has been introduced into the coordination core an additional spin delocalization mechanism has been found to be instrumental. This new delocalization route is remarkably effective. The sign of spin densities at meso positions of **5** and **6** is identical as for (TPP)Fe^{III}Cl,[52] which results in the upfield position of *ortho*-H and *para*-H resonances and, respectively, the downfield shifts for meta protons. Significantly, the reversed signs of the meso spin densities for **3** and **4** have been determined as reflected by the reversed shift signs of *meso*-aryl resonances. (Figures 4-6, Table 1S and 2S—see the Supporting Information). In qualitative terms one can readily assume that the unique (CO)···Fe route provides the negative spin π density meso carbons of **3** and **4**. A detailed analysis requires a more advanced description of electronic structure for **3** and **4**.

Another characteristic feature of the iron(III) complexes **5** and **6** is the localized effect of the *N*-confused pyrrole ring. For **5** and **6** one pyrrole and 2-NH resonances are clearly distinct from the other six and show a considerable upfield shift. The logical conclusion is that the side-on-location of the iron(III) with respect to the pyrrole ring primarily affects spin transfer to the modified pyrrole ring. The inverted pyrrole reflects the features of side-on interaction described for heteroporphyrins.[4,12] In addition one can expect some contribution of an agostic interaction as discussed previously for **1**.[39]

The isotropic shift pattern for β-H pyrrole of **2** and **7** reflects the extensive spin delocalization into π molecular orbitals of inverted porphyrin. The dominance of the π-spin transfer mechanism has been taken as a direct evidence that $d_{x^2-y^2}$ is not populated in **2** and **7**. Thus, the ground state can be related to the following models of the electronic configuration: intermediate-spin $(d_{xy})^2(d_{xz})^1(d_{yz})^1(d_{z^2})^1(d_{x^2-y^2})^0$ for **2** and low-spin $(d_{xy})^2(d_{xz}d_{yz})^3(d_{z^2})^0(d_{x^2-y^2})^0$ for **7**. The intermediate $S = 3/2$ ground electronic state is characterized by the upfield shift similarly as the low spin one as the identical delocalization path is operating.[45] The β-H shift value is expected to be large as there are two π-symmetry unpaired electrons in the $S = 3/2$ state in comparison to one for $S = 1/2$ as clearly exemplified the **2** and **7** couple.[80]

Conclusion

An insertion of the oxygen atom into the M−C bond (a carbon atom built into the aromatic moiety) is quite rare.[41,83−91] In particular, the dioxygen addition to (P)Fe^{III}Ar yielded the phenoxide complexes, (P)Fe^{III}OAr as the principle products.[41,92] The corresponding alkyl complexes (P)Fe^{III}R (P, porphyrin dianion; R, alkyl group) reacted with dioxygen to form intially μ-peroxo complexes (P)Fe^{III}OOR trapped in low temperatures. This intermediates decomposed to (P)Fe^{III}OH and an aldehyde, ketone or alcohol when R was a primary, secondary, or tertiary alkyl group.[40]

The results reported here demonstrate that dioxygen reacts cleanly with iron(II) 2-aza-21-carbaporphyrin to form the corresponding five-coordinate intermediate-spin iron(III) complexes and eventually, 2-aza-21-carbaporphyrin gains the oxo functionality. No direct evidence for the formation of intermediates in the oxygenation process has been found. An oxygenation mechanism has been considered which involves the insertion of dioxygen molecule into the Fe−C bond to form a transient Fe−O−O−C(21) peroxide. A rapid O−O bond cleavage results in a unique situation where two reactive centers are locked in the macrocyclic cage as a consequence of restraints imposed by the ligand structure. Further investigations of the iron carbaporphyrinoid complexes are expected to afford an insight into the reactivity of a metal−carbon bond as specifically tuned carbaporphyrins can be expected to stabilize intermediates of the oxygenation process.

Experimental Section

Materials. Inverted porphyrin (CTPP*H*)H$_2$ and its iron(II) complexes (*H*CTPP*H*)Fe^{II}Br have been obtained by already described methods.[25,93] The deuterated derivatives have been synthesized using pyrrole-d_5 or benzaldehyde-d_6 in condensation.[12] Chloroform-*d* used in ^{1}H NMR was deacidified by passing down a basic alumina column. Toluene-d_8, dichlo-

(80) Balch, A. L.; Cheng, R.-J.; La Mar, G. N.; Latos-Grażyński, L. *Inorg. Chem.* **1985**, *24*, 2651.
(81) Wojaczyński, J.; Latos-Grażyński, L.; Hrycyk, W.; Pacholska, E.; Rachlewicz, K.; Szterenberg, L. *Inorg. Chem.* **1996**, *35*, 6861.
(82) Cheng, R.-J.; Chen, P.-Y.; Lovell, T.; Liu, T.; Noodleman, L.; Case, D. A. *J. Am. Chem. Soc.* **2003**, *125*, 6774.
(83) Grigor, B. A.; Neilson, A. *J. Organomet. Chem.* **1977**, *129*, C17.
(84) Kamaraj, K.; Bandyopadhyay, D. *J. Am. Chem. Soc.* **1997**, *119*, 8099.
(85) Wadhwani, P.; Mukherjee, M.; Bandyopadhyay, D. *J. Am. Chem. Soc.* **2001**, *123*, 12 430.
(86) Ryabov, A. D. *Synthesis* **1985**, 233.
(87) Mahapatra, A. K.; Bandyopadhyay, D.; Bandyopadhyay, P.; Chakravorty, A. *Inorg. Chem.* **1986**, *25*, 2214.
(88) Sinha, C.; Bandyopadhyay, D.; Chakravorty, A. *Inorg. Chem.* **1988**, *27*, 1173.
(89) Chattopadhyay, S.; Sinha, C.; Basu, P.; Chakravorty, A. *Organometallics* **1991**, *10*, 1135.
(90) Marsella, A.; Agapakis, S.; Pinna, F.; Strukul, G. *Organometallics* **1992**, *11*, 3578.
(91) Valk, J.-M.; Boersma, J.; van Koten, G. *Organometallics* **1996**, *15*, 1996.
(92) Balch, A. L.; Hart, R. H.; Latos-Grażyński, L. *Inorg. Chem.* **1990**, *29*, 3253.
(93) Geier, G. R., III.; Haynes, D. M.; Lindsey, J. S. *Org. Lett.* **1999**, *1*, 1455.

romethane-d_2, chloroform-*d*, DMSO-d_6, DMF-d_7 were degassed by freezing-pumping-thawing method and stored in a dry glovebox.

^{1}H NMR Studies and Low-Temperature Studies. The solution of (*H*CTPP*H*)Fe^{II}Br in a deuterated solvent was prepared under purified nitrogen in a glovebox. The sample concentration **1** in the solvent of choice were on the order 2−5 mM Thus, typically a sample ca. 1−2 mg of **1** was dissolved in 0.5 mL of deuterated solvent. The solution was directly placed into an ^{1}H NMR tube and sealed with a septum cap. In titration experiments, a solution of the appropriate nitrogen base or oxidizing reagent in the deuterated, deoxygenated solvent was gradually added to the sample through a 10-μL microsyringe. Usually, an appropriate mass of an applied reagent was dissolved to give an approximately 0.25 M solution. It typically required 2−5 μL of the solution to be added to the NMR tube containing iron inverted porphyrin to cause a detectable conversion. A stepwise addition of dioxygen was carried out by titration with the deuterated solvent saturated with dioxygen.

In the case of low-temperature studies, the sample was removed from the glovebox and cooled to 195 K in the ethanol bath which was chilled by the addition of sufficient amount of liquid nitrogen to reach 195 K. Dioxygen was introduced into the sample through the syringe needle. The sample was shaken in the cold bath and transferred to the precooled NMR probe and the progress of the reaction was followed by ^{1}H NMR spectroscopy.

^{2}H NMR Studies. The samples used in ^{2}H NMR experiments have been prepared similarly as for ^{1}H NMR starting from (*H*CTPP*D*-d_7)Fe^{II}Br and using regular solvents.

Solution Magnetic Moment Measurements.[43] The magnetic susceptibility data carried out for five samples in the concentration range 2.7 mg/mL to 3.6 mg/mL. The measurements were carried out in chloroform-*d* using methylene chloride as an internal reference. After the completion of Evans method measurement on (*H*CTPP*H*)Fe^{II}Br **1**, the solution was exposed briefly to dioxygen and the ^{1}H NMR spectra were recorded to trace the progress of the reaction. The measurements of (*H*CTPP)Fe^{III}Br **2** were made when no (*H*CTPP*H*)Fe^{II}Br **1** and [(CTPP*O*)Fe^{III}Br]$^-$ **3** ^{II}Br were observable in ^{1}H NMR spectra. The measurements gave the following magnetic moments: 4.87 ± 0.10 μ_B for (*H*CTPP*H*)Fe^{II}Br and 4.19 ± 0.10 μ_B for (*H*CTPP)Fe^{III}Br. The solution magnetic moment of [(CTPP*O*)Fe^{III}Br]$^-$ **3** (5.6 ± 0.1 μ_B) was also determined starting from the separately synthesized compound (*H*CTPP*O*)Fe^{III}Br **4**. Diamagnetic correction of ligand was made using the value of 409 × 10^{-6} cgs emu/mol calculated from Pascal's constants.

Instrumentation. ^{1}H NMR (300 and 500 MHz) spectra were measured on Bruker AMX 300 and Bruker Avance 500 spectrometers. The peaks were referenced against the residual resonances of the deuterated solvents. The ^{2}H NMR spectra were collected using a Bruker Avance 500 instrument operating at 76.77 MHz. A spectral width of 200 ppm was typical and 16 K points was used. A pulse delay of 50 ms was applied. The residual ^{2}H NMR resonances of the solvents were used as a secondary reference.

The mass spectra were obtained on the Finnigan MAT TSQ 700 spectrometer by means of ESI method. UV−vis spectra were recorded on the Hewlett-Packard 8435 diode-array spectrophotometer. IR spectra were measured on the FTIR−IFS 113 V Bruker spectrometer.

Table 3. Summary of Crystallographic Data (*H*CTPP)Fe^{III}Br **2** and (*H*CTPP*O*)Fe^{III}Br **4**

	2	**4**
empirical formula	$C_{44}H_{28}BrFeN_4$	$C_{51}H_{36}BrFeN_4O$
formula weight	748.46	856.60
temperature	298(2) K	150(2) K
crystal system	monoclinic	monoclinic
space group	$P2_1/n$	$C2/c$
a, Å	10.288(2)	33.229(4)
b, Å	15.757(3)	13.2249(15)
c, Å	20.811(4)	18.102(2)
b	90.000(4)°	94.060(2)°.
V, Å^3	3373.5(11)	7935.0(15)
Z	4	8
D_{calcd}, g·cm^{-3}	1.474	1.434
absorption coefficient	1.671 mm^{-1}	1.433 mm^{-1}
θ range	1.62 to 25.08°	1.23 to 27.52°.
hkl ranges	−11 to 12, −18 to 17, −22 to 24	−30 to 43, −16 to 17, −22 to 23
reflections collected	17738	24572
independent reflections	5961 [*R*(int) = 0.1215]	9062 [*R*(int) = 0.0914]
parameters	451	498
goodness-of-fit on F^2	0.583	1.034
*R*1/*w*R2 [*I* > 2sigma(*I*)][a]	0.0449/0.0910	0.0510/0.1043
*R*1/*w*R2 (all data)	0.2401/0.1586	0.1616/0.1606
max/min peak (e.Å^{-3})	0.268/0.366	0.900/−0.660

[a] $R1 = \Sigma||F_o| - |F_c||/\Sigma|F_o|$. $wR2 = [\Sigma[w(F_o^2 - F_c^2)^2/\Sigma[w(F_o^2)^2]\}^{1/2}$.

Isolation of (*H*CTPP)Fe^{III}Br 2 and (*H*CTPP*O*)Fe^{III}Br 4. (*H*CTPP)Fe^{III}Br 2. In a round-bottom flask, (*H*CTPP*H*)Fe^{II}Br (100 mg, 0.133 mmol) was dissolved in 30 mL of anhydrous CH_2Cl_2. The solution was exposed to air for one minute. The green solution was then capped and stirred at room temperature. The progress of the reaction was monitored by UV−vis spectroscopy and the reaction was stopped when the peak at 461 nm completely disappeared. After solvent removal under vacuum the product was placed in the inner atmosphere drybox. The solid was recrystallized from THF/hexane under anaerobic condition to obtain crystals suitable for X-ray analysis. The yield of this reaction is near quantitative. Anal. Calcd for $FeBrN_4C_{44}H_{28}\cdot 0.1THF\cdot 0.3CH_2Cl_2$: N, 7.17; C, 68.73; H, 3.79. Found: N, 6.59; C, 68.80; H, 3.28. UV−vis (CH_2Cl_2) [λ_{max}, nm (log ϵ, M^{-1} cm^{-1})]: 337 (4.51), 361 (4.50), 416 (4.48), 564 (4.09), 692 (3.49), 887 (3.60).

(*H*CTPP*O*)Fe^{III}Br 4. (*H*CTPP*H*)Fe^{II}Br (50 mg, 0.067 mmol) was dissolved in 30 mL of anhydrous CH_2Cl_2. The solution was bubbled with oxygen for one minute. The green solution was then capped and stirred at room temperature for 12 h. The progress of the reaction was monitored by UV−vis spectroscopy and the reaction was stopped when the Soret band shifted to 390 nm and *Q* band of the starting (*H*CTPP*H*)Fe^{II}Br disappeared. After solvent removal under vacuum the product was placed in the inner atmosphere drybox. The crude solid was dissolved in 3 mL of CH_2Cl_2 and a slow addition of hexane precipitated the desired product. Yield: 39 mg (76%). The crystals suitable for X-ray analysis were obtained from a slow diffusion of hexane into a toluene solution of **4**. Anal. Calcd for $FeBrN_4C_{44}H_{28}O$: N, 7.33; C, 69.13; H, 3.69. Found: N, 7.35; C, 68.81; H, 3.97. UV−vis (CH_2Cl_2) [λ_{max}, nm (log ϵ, M^{-1} cm^{-1})]: 390 (4.76), 572 (3.99, sh), 670 (3.82, sh).

Crystallography Studies. The crystal of (*H*CTPP)Fe^{III}Br **2** were obtained from a slow diffusion of *n*-hexane into a THF solution of **2** under anaerobic conditions. The crystal of (*H*CTPP*O*)Fe^{III}Br **4** were obtained from a slow diffusion of

n-hexane into a toluene solution of **4** under anaerobic conditions. The summary of crystallographic data is given in Table 3.

Each crystal was attached to the tip of a glass capillary and mounted on a Bruker SMART 1000 CCD diffractometer for data collection using graphite-monochromated MoKα (λ = 0.710 73 Å) radiation. All non-hydrogen atoms were refined anisotropically, and hydrogen atoms were placed in ideal positions and refined as riding atoms with relative isotropic displacement parameters. The N2 and C3 of compound **4** were refined as mutually disorder with 50% occupancy on each site. The coordinates and thermal parameters were defined equated on the two atoms sharing the same site. In the crystal lattice, there are two independent toluene sites with half occupancy on each site. The atoms on the phenyl ring of the disordered toluenes were constrained to regular hexagonals and refined isotropically.

Acknowledgment. This work was supported at the University of Wrocław by the State Committee for Scientific Research KBN of Poland (Grant 4 T09A 147 22) (L.L.-G.) and by the National Science Council of Taiwan (C.-H.H.).

Supporting Information Available: Crystallographic data for **2** and **4** (CIF), the figure showing packing and intermolecular interactions in the crystal lattice of (*H*CTPP*O*)Fe^{III}Br **4**, VT NMR data for **2**, **3**, **4**, **5**, **6**, tables of chemical shifts of *meso*-phenyl resonances for **3**, **4**, **5**, and **6**. This material is available free of charge via the Internet at http://pubs.acs.org.

JA039792Y